Enhancing UGV Path Planning using Dynamic Bayesian Filtering to Predict Local Minima

by

Seung Hun Lee

A thesis submitted in partial fulfillment
of the requirements for the degree of
Master of Science
(Electrical Computer Engineering)
in the University of Michigan
2024

Doctoral Committee:

Professor Dawn M. Tilbury, Chair
Professor Lionel P. Robert Jr.
Professor Necmiye Ozay


MAVRIC

Seung Hun Lee
armyhuni@umich.edu
ORCID iD: 0009-0008-1037-087X

ACKNOWLEDGEMENTS

I must express my deepest gratitude to the organizations whose support and resources have been pivotal in my pursuit of a Master's degree and the completion of this work: the Republic of Korea Army Military Headquarters; the Department of Electrical and Computer Engineering at the University of Michigan; the Automotive Research Center (ARC); and the United States Army Combat Capabilities Development Command/Ground Vehicle Systems Center (GVSC).

I am equally thankful for the camaraderie and support from my MAVRIC lab members: Wonse Jo, Connor Esterwood, Arsha Ali, Zariq George, and Hongziao Qiang.

My profound gratitude goes to my advisors, Professor Dawn Tilbury, Professor Lionel Robert, and Professor Necmiye Ozay, for their immense support. They have challenged me significantly, contributing to the submission of the ARC proposal and advancing research on off-road path planning. They have done their utmost to teach me how to conduct high-quality research.

Above all, my heartfelt thanks go to my incredible family. To my parents, for their boundless love and support; and to my brother, for being an invaluable friend.

TABLE OF CONTENTS

ACKNOWLEDGEMENTS ii

LIST OF FIGURES iv

LIST OF TABLES v

ABSTRACT vi

CHAPTER

1 Introduction **1**

2 Background **4**

2.1 Artificial Potential Field (APF) 4
2.2 Discrete Time Control 5

3 Local Minima Prediction **8**

3.1 Introduction 8
3.2 Methodology 9
3.2.1 Dynamic Bayesian Filtering 12
3.2.2 Prediction Step 13
3.2.3 Correction Step 14
3.2.4 Normalization 15
3.3 Simulation Environment 16
3.4 Results 17
3.4.1 Comparison Methods 17
3.4.2 A Novel Dynamic Bayesian Filtering Method 18

4 Discussion **20**

4.1 Contributions and Implications 20
4.2 Limitations and Future Work 21

5 Conclusion **22**

APPENDICES 23

BIBLIOGRAPHY 25

LIST OF FIGURES

FIGURE

1.1 Two common situations where local minima in artificial potential fields arise. . 3

2.1 UGV Navigation in APF (A Bird's-Eye View). 7

3.1 AOI, RA(X_{t_0}), and UA(X_{t_0}) Figures. 10
3.2 Occupied Points Angle. 14
3.3 Two Occupancy Simulation Environments 16
3.4 Two Comparision Methods. (Method I: Left Figure, Method II: Right Figure) . 17
3.5 Belief in Local Minimum: Two Cases. 19

LIST OF TABLES

TABLE

3.1 Results: Comparison Methods 18
3.2 Results: A Novel Approach 19

ABSTRACT

Path planning is crucial for the navigation of autonomous vehicles, yet these vehicles face challenges in complex and real-world environments. Although a global view may be provided, it is likely to be outdated, necessitating the reliance of Unmanned Ground Vehicles (UGVs) on real-time local information. This reliance on partial information, without considering the global context, can lead to UGVs getting stuck in local minima. Obstacles beyond the known or locally-sensed areas can result in inaccurate predictions of local minima. This thesis focuses on proactively predicting these local minima using Dynamic Bayesian filtering, based on the detected obstacles in the local view and the global goal. This approach aims to enhance the autonomous navigation of self-driving vehicles by allowing them to predict potential pitfalls before they get stuck.

CHAPTER 1

Introduction

Autonomous vehicles are becoming increasingly prevalent on our city streets, and their underlying technology also has military applications in the realm of Unmanned Ground Vehicles (UGVs). Recent urban incidents have highlighted the challenges of navigating in real, complex, and unknown environments, as these "self-driving" cars often grapple with and can get stuck in anomalous traffic scenarios [19]. Significant concerns arise with an over-reliance on autonomy in complex terrains. Such complex settings contrast sharply with global navigation, which leans heavily on pre-mapped and stable environments [3]. However, local path planning techniques such as the Vector Field Histogram (VFH), and Dynamic Window Approach (DWA) have gained prominence for their capacity to respond in real-time to unforeseen obstacles within the sensory range [12]. Studies underscore how UGVs employ techniques such as Artificial Potential Fields (APF) to create obstacle-free paths, attributing positive "charges" to distant goals and negative ones to nearby obstacles, thus providing a computationally efficient and practical solution for many navigation scenarios [6, 16, 18]. While a UGV can autonomously generate a path using the APF, it faces three significant challenges: becoming trapped in local minima when confronted with an obstacle, difficulty navigating between obstacles, and experiencing undesirable oscillations [2, 9, 15]. Among these challenges, encountering local minima may particularly lead to a failed mission, as the UGV halts its navigation before reaching the goal position. Therefore, predicting the local minima is increasingly important for UGV navigation.

To predict the local minima, some studies have assumed a well-defined environment, such as fully mapped or convex settings [7, 11]. While these methods can identify the local minima, practical applications require not only the assumption of a known environment but also the preprocessing stage: dilation of obstacles and transformation to convex-shaped obstacles [14]. This stage entails the transformation of non-convex terrain into simplified and convex shapes, which might result in distortion of the environment. In contrast, other research has focused on adapting to non-convex environments, which are more closely aligned with the complexity of real environments [15, 16]. To predict local minima, these studies have concentrated on specific shapes, such as triangular or U-shaped, which can be challenging to apply in a general context. Moreover, their prediction of the local minima might be incorrect since undiscovered obstacles in unknown areas can lead to incorrect predictions.

Navigating in an off-road environment, the UGV faces significant challenges in recognizing the surrounding environment [10]. We assume that the UGV relies on a sensor that provides values indicating distance to obstacles such as rocks, fallen logs, and bushes, without discerning their semantic meanings. Therefore, the UGV can only differentiate between free space, where it can maneuver, and obstacles, which it considers impassable. This limited perception framework lays the groundwork for our study, aiming to predict the occurrence of local minima in advance within an environment that is only partially known. Given that the UGV is aware of its current position and the goal, we also assume that it navigates towards the goal using its local view and a fixed step size within an APF field. There exist an attractive force ($\vec{F}_{\text{att}}$) towards the goal and repulsive forces ($\vec{F}_{\text{rep}}$) from locally observed obstacles. For prediction, we have defined a state transition model that uses raw sensor data which indicates obstacle positions or free space within the sensor range. We also consider the uncertainty of the information in its current state to refine the prediction. We demonstrate the superiority of our methodology by comparing its prediction results with those from other methods in two common situations where local minima arise (see Figure 1.1).

In sum, the contributions of this thesis are (i) a novel method that estimates the proba-

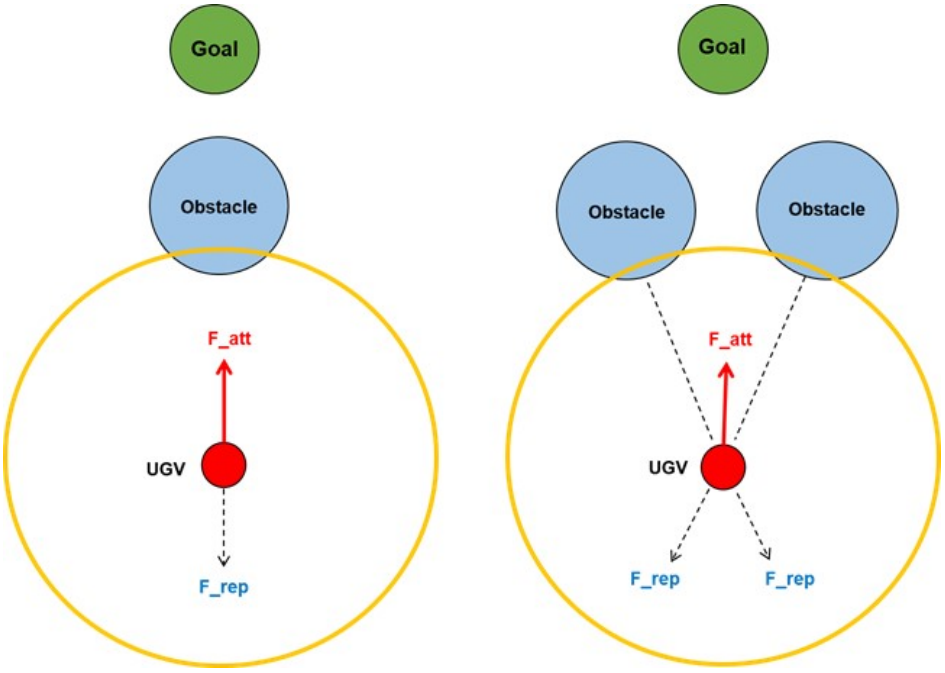

Figure 1.1: Two common situations where local minima in artificial potential fields arise.

bility of the UGV becoming trapped in local minima and (ii) outperforms existing models in predicting local minima in APF. A brief background of previous work done in APF local path planning is discussed in Chapter 2. The proposed method for local minima prediction, the simulation setup, and the results are detailed in Chapter 3. Finally, the discussion and conclusion are provided in Chapters 4 and 5, respectively.

CHAPTER 2

Background

2.1 Artificial Potential Field (APF)

The Artificial Potential Field (APF) algorithm operates by considering the sum of virtual forces generated by external elements, such as the goal position or obstacles, to determine the motion of a UGV [5]. The UGV computes an $\vec{F}_{\text{att}}$ from the goal position, as well as $\vec{F}_{\text{rep}}$ from nearby obstacles.

$$\begin{aligned}\vec{F}_{\text{att}}(t) &= \xi(X(t) - X_g) \\ \vec{F}_{\text{rep}}(t) &= \sum_{i=1}^{S(t)} \eta \frac{1}{||\vec{d_i}(t)||^2} \left(\frac{1}{||\vec{d_i}(t)||} - \frac{1}{\rho_0} \right) \frac{\vec{d_i}(t)}{||\vec{d_i}(t)||}\end{aligned} \tag{2.1}$$

where $X(t)$ is the UGV's current position at time t, X_g is the goal position, ρ_0 is the sensor range, $S(t)$ is the set of discovered obstacles in sensor range at time t, $\vec{d_i}(t)$ is the vector from UGV to the ith obstacle in $S(t)$, ξ is the coefficient of $\vec{F}_{\text{att}}(t)$, and η is the coefficient of $\vec{F}_{\text{rep}}(t)$.

These virtual forces enable the UGV to reach the goal position by steering it away from obstacles, thereby preventing collisions. The magnitude and direction of these forces depend on the locations of both the goal position and the obstacles. By combining these forces, the UGV is guided away from obstacles while maintaining a safe distance. However, the APF

algorithm faces a local minima challenge that occurs when the forces $\vec{F}_{\text{att}}$ and $\vec{F}_{\text{rep}}$ sum to zero.

Various methodologies have been reported to predict local minima. However, previous research has limitations in predicting local minima since it requires a known or restricted environment that may not be realistic. Some research has implemented harmonic potentials based on the principle that potential flows in incompressible fluids adhere to Laplace's equation [4, 7, 8]. Other research has focused on predicting local minima in fully known or convex environments. Several groups created a convex potential field environment and defined the navigation function to avoid local minima [11, 14, 17]. One research found that there is one unique attractor at the goal location and one local minimum point associated with each obstacle among the stationary points in known convex sphere worlds [1]. In contrast, recent research has focused on non-convex environments, which resemble complex and realistic settings. One recent research predicted the local minima from the U-shaped obstacle by using the shape of a LiDAR sensor's range or from the triangular shape by using the horizon of a LiDAR sensor [15, 16]. However, this method is difficult to generalize for all shapes and real-world environments and fails to account for unknown areas when updating the prediction since the prediction in local path planning will become more accurate as more information becomes available.

2.2 Discrete Time Control

The APF method simplifies the control problem by translating complex environmental interactions into straightforward force vectors. Therefore, the state of the UGV at time t is $X(t) = [x_t, y_t]$. We assumed the UGV is moving on a plane where the UGV's elevation is constant. At each time t, the UGV moves a distance Δ in the direction of $\vec{F}_{\text{tot}}(t) = \vec{F}_{\text{att}}(t) - \vec{F}_{\text{rep}}(t))$, as defined in Eq. (2.1).

Algorithm 1 Artificial Potential Field

Definitions:
X_g: the goal position (known)
Local Info.(t): the local information indicating distance to obstacles in sensor range
$S(t)$: the set of obstacles $(O^1, \ldots, O^k)$ in Local Info.(t)
O^i: the i^{th} obstacle in $S(t)$
P_i: the set of occupied points which shapes O^i
ρ_0: the radius of the sensor range

Start: Given X_g, $X(t)$, and Local.Info(t)

while $\|X_g - X(t)\| > 0.1$ **do**
Sense the Local Info.(t)
for j = 0 to 99 **do**

$$d_{\theta_j} = \begin{cases} \rho_{\theta_j} & \text{if obstacle exists} \\ \rho_0 & \text{otherwise} \end{cases}$$

$$z_t^j = \begin{cases} 1 & \text{if } d_{\theta_j} < \rho_0 \\ 0 & \text{if } d_{\theta_j} = \rho_0 \end{cases}$$

end for

Mapping the binary values to Observation $z_t = [z_t^0, z_t^1, \ldots, z_t^{99}]^T$

Let $D = \{d_{\theta_j}\}$
for i = 1 to k **do**
Let $P_i = \min_j D$
Add to P_i surrounding points $d_{\theta_j \pm 1 \ldots}$ where $z_t^j = 1$
Set $D \leftarrow D \backslash P_i$
end for

Compute $\vec{F}_{\text{tot}}(t)$
$\vec{F}_{\text{att}}(t), \vec{F}_{\text{rep}}(t)$ according to equation (2.1)
$\vec{F}_{\text{tot}}(t) = \vec{F}_{\text{att}}(t) + \vec{F}_{\text{rep}}(t)$

Move to next position $X(t+1)$
$X(t+1) = X(t) + \Delta \times \frac{\vec{F}_{\text{tot}}(t)}{\|\vec{F}_{\text{tot}}(t)\|}$

end while

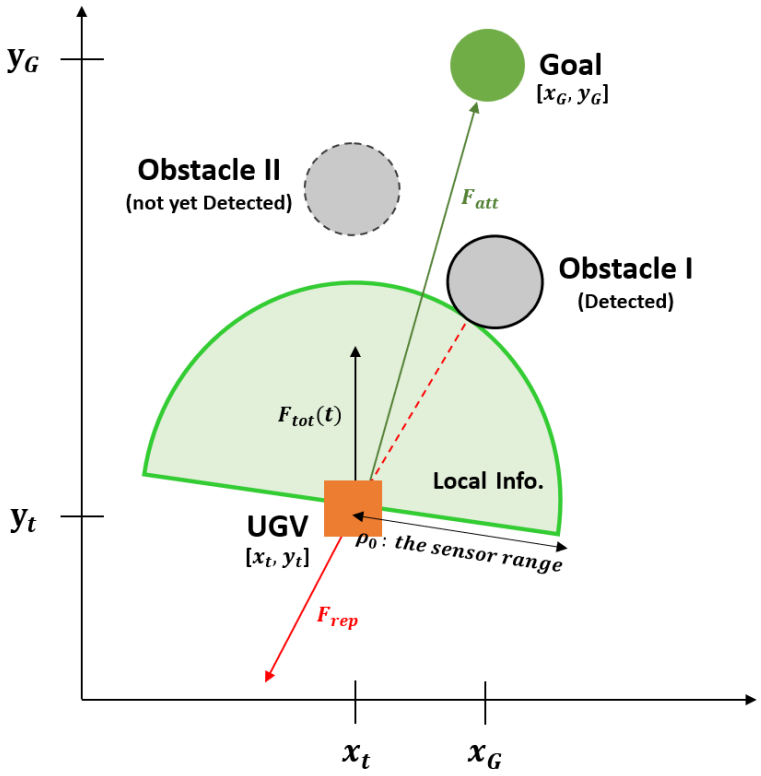

Figure 2.1: UGV Navigation in APF (A Bird's-Eye View).

$$x_{t+1} = x_t + \cos\left(\tan^{-1}\left(\frac{\vec{F}_{\text{tot},y}}{\vec{F}_{\text{tot},x}}\right)\right) \times \Delta$$
$$y_{t+1} = y_t + \sin\left(\tan^{-1}\left(\frac{\vec{F}_{\text{tot},y}}{\vec{F}_{\text{tot},x}}\right)\right) \times \Delta \tag{2.2}$$

CHAPTER 3

Local Minima Prediction

3.1 Introduction

In the APF framework, the UGV can get stuck in a local minimum and be unable to move toward its goal autonomously, as the total force vector $\vec{F}_{\text{tot}}(t)$ may become zero when the UGV is following the Algorithm 1.

Definition 1 (Local Minimum (X_{lm})) *The local minimum (X_{lm}) is a position where the attractive force ($\vec{F}_{att}(t)$) and the repulsive force ($\vec{F}_{rep}(t)$) are balanced out i.e. the total force vector $\vec{F}_{tot}(t)$ is zero.*

A necessary condition for a local minimum to exist is that $\vec{F}_{\text{att}}(t)$ and $\vec{F}_{\text{rep}}(t)$ are parallel. If the UGV moves along $\vec{F}_{\text{tot}}(t)$ towards the goal, it may encounter a minimum point where the forces are equal and opposite (but non-zero). However, as the UGV moves along $\vec{F}_{\text{tot}}(t)$, it is able to sense further and could encounter another obstacle that would add to the repulsive force (see Obstacle II in Figure 2.1). Newly identified obstacles will break the parallelism, so local minima may not exist as predicted in previous steps. Therefore, the presence of obstacles in unknown areas is important to consider when predicting a local minimum. In this paper, we assume the UGV is moving toward its goal with a sensor oriented in the UGV's heading direction and navigating an environment with unknown obstacles on its path. At each time step t, it can sense an area in front of it, identifying obstacles within a defined

radius. Using this Local.Info and the location/direction of obstacles, it can compute $\vec{F}_{\text{rep}}(t)$. If $\vec{F}_{\text{att}}(t)$ and $\vec{F}_{\text{rep}}(t)$ are parallel, then the proposed method of estimating a local minimum is invoked.

In this chapter, we propose a novel approach for predicting local minima during navigation in APF by using Dynamic Bayesian filtering. In Section 3.2, we introduce the conditions where the local minimum occurs in APF. In addition, we explain how the area information can be described based on the sensing area observed by the UGV. Moreover, we demonstrate how the belief of a local minimum can be recursively updated using this area information. In the following sections, we explain the simulation environment that we constructed for UGV local path planning within APF. We also demonstrate the superiority of our methodology by comparing its prediction results with those from two other previous methods in two common situations where local minima arise.

3.2 Methodology

As the UGV traverses along the APF, if no further obstacles are detected, the local minimum will either be predicted in advance, or eventally reached. In this case, the higher-level planning algorithm can attempt an avoidance maneuver. If more obstacles are detected, the parallelism of the attractive and repulsive vectors could be broken, and a local minimum will not occur, and the UGV can continue traversing towards the goal along the APF.

Definition 2 (Sensing Area (SA(X))) *An area equivalent to Local info.(t) when the UGV is positioned at X(t) (See Figure 2.1).*

Definition 3 (Area Definitions) *In the case when the attractive and repulsive forces are parallel, three distinct areas are defined in relation to the UGV's navigation and obstacle detection capabilities:*

- ***Area of Interest (AOI)**: An area that encompasses from $RA(X_{t_0})(= SA(X_{t_0}))$ to $SA(X_{lm})$ (i.e. $\bigcup_{X=X_{t_0}}^{X_{lm}} SA(X)$).*

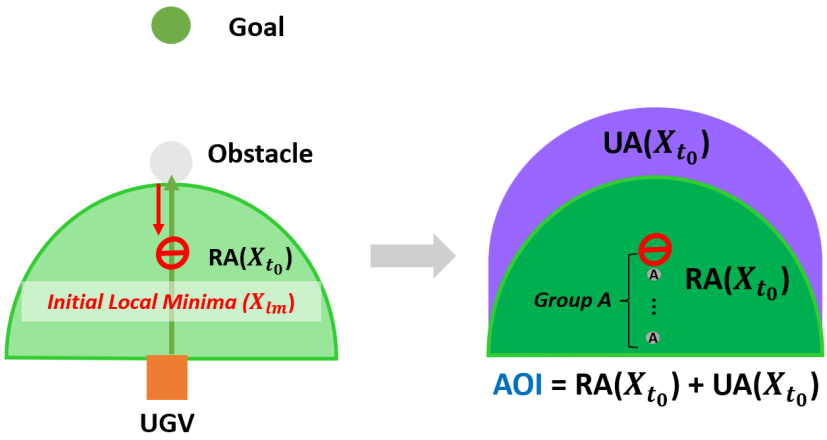

Figure 3.1: AOI, RA(X_{t_0}), and UA(X_{t_0}) Figures.

- ***Recognized Area (RA(X_t))****: An area in AOI that is recognized by the UGV up to time t (i.e.* $\bigcup_{X=X_{t_0}}^{X_t} SA(X)$*).*
- ***Unknown Area (UA(X_t))****: An area within AOI that has not been recognized by the UGV at time t.*

To clarify which areas are known or unknown at time t, we categorize the area around the UGV into three distinct zones: the Area of Interest (AOI), the Recognized Area (RA(X_t)), and the Unknown Area (UA(X_t)). First, the AOI is identified after $\vec{F}_{\text{att}}(t)$ and $\vec{F}_{\text{rep}}(t)$ are parallel at time t_0, indicating that a local minimum is likely to appear within the AOI. Second, the RA(X_t) is the area within which the UGV can detect obstacles and free spaces for maneuvering up to time t, and it increases as the UGV moves forward. Lastly, the UA(X_t) is an area within the AOI that the UGV cannot recognize at time t, and it decreases over time after t_0. In the UA(X_t), undiscovered obstacles may cause the UGV to encounter local minima sooner or allow it to maneuver toward the goal without encountering the initial local minima within a few steps.

In Algorithm 2, we can identify the initial X_{lm}, where $\vec{F}_{\text{tot}}(t)$ is predicted to be zero in RA(X_{t_0}) if no other obstacles are encountered. Moreover, by dividing the line between the UGV and the initial X_{lm}, we can generate potential points, denoted as Group A. The points

Algorithm 2 Local Minima Prediction

Assume $\vec{F}_{\text{att}}(t)$ and $\vec{F}_{\text{rep}}(t)$ are parallel at time t_0, when the UGV is at X_{t_0}

(Initialization Step, see Figure 3.1)

$RA(X_{t_0}) \leftarrow Local\ Info.(t_0)$
$X_{lm} \leftarrow$ the projected point where $F_{tot} = 0$
$SA(X_{lm}) \leftarrow$ UGV could observe from X_{lm}
$AOI \leftarrow RA(X_{t_0}) \cup SA(X_{lm})$
Generate Group A
Define initial belief $bel_{t_0}(X_{lm})$

(Recursive Step)

while $bel_t(X_{lm}) < \gamma$ **do**

1. Prediction Step:

Update $\bar{bel}(X_{lm})$ by multiplying state transition probability (Definition 4)

2. Correction Step:

Refine $bel(X_{lm})$ by multiplying observation likelihood (Definition 5)

3. Normalization Step:

Adjust $bel(X_{lm})$ by multiplying normalization factor ν

if $bel(X_{lm}) < \gamma$ at time t **then**
$t \leftarrow t + 1$
UGV move one step to $X(t+1)$ along $\vec{F}_{tot}$
else
break
end if

end while

Report: "UGV is likely to get stuck in X_{lm} with $\gamma \times 100\%$ confidence level."

outside Group A, which lie between the obstacle and the initial local minimum, represent points where the UGV cannot maneuver within the APF field, as $\vec{F}_{\text{rep}}(t)$ from the obstacles outweighs $\vec{F}_{\text{att}}(t)$. However, Group A comprises points between the initial local minimum and the UGV, including the local minimum itself, where the UGV may be able to maneuver within the APF field since $\vec{F}_{\text{att}}(t)$ exceeds $\vec{F}_{\text{rep}}(t)$. These points are likely to become local minima unless the UGV encounters undetected obstacles that change the direction of $\vec{F}_{\text{rep}}(t)$ in the UA(X_t). Therefore, we can define the initial belief ($bel_{t_0}(X_{lm})$), which represents the probability that the initial X_{lm} could be the local minimum among the points in Group A.

$$bel_{t_0}(X_{lm}) = \frac{1}{|\text{Group A}|} \tag{3.1}$$

where |Group A| is the number of points in Group A. As noted in Chapter 4, there may be other ways to define this initial belief.

3.2.1 Dynamic Bayesian Filtering

In Dynamic Bayesian filtering [13], the filtering process involves three sequential steps: prediction, correction, and normalization under the Markov Assumption (Assumption 1). The prediction step uses the system's prediction model to forecast the subsequent state by incorporating the state transition probabilities and the prior belief from the previous time step. In the correction step, the prediction is refined with the latest observations z_t (i.e. the UGV perceives a local minimum as such in RA(X_t)) by computing the likelihood of the new observation given the predicted state, resulting in a corrected posterior belief. Finally, the normalization step adjusts the posterior belief so that the sum of the probabilities equals one, thus maintaining a valid probability distribution (see Appendix).

Assumption 1 (Markov Assumption) *Given a sequence of observations $z_1, z_2, \ldots, z_n$ and X_{lm}, the observation z_n is conditionally independent of all previous observations*

$z_1, z_2, \ldots, z_{n-1}$ *given* X_{lm}*. Or equivalently we can state:*

$$\begin{aligned} p(X_{lm}|z_1, \ldots, z_n) &= \frac{p(z_n|X_{lm})p(X_{lm}|z_1, \ldots, z_{n-1})}{p(z_n|z_1, \ldots, z_{n-1})} \\ &= \eta_n p(z_n|X_{lm})p(X_{lm}|z_1, \ldots, z_{n-1}) \\ &= \eta_{1:n} \prod_{i=1}^{n} p(z_i|X_{lm})p(X_{lm}) \end{aligned}$$

where $\eta_{1:n}$ *is defined as the product of normalization constants* $\eta_1\eta_2 \cdots \eta_n$*, ensuring that probabilities sum to one.*

3.2.2 Prediction Step

Definition 4 (State Transition Probability) *The state transition probability, denoted by* $P(X_{lm}^t \mid X_{lm}^{t-1}, z_{1:t-1}, u_{1:t})$*, represents the probability of the status (being a local minimum) of* X_{lm} *at time* t *given its status at time* $t-1$*, the sequence of all observations up to time* $t-1$*, and the sequence of all inputs up to time* t*. The input* u_t *indicates that the UGV follows the total force* $\vec{F}_{tot}(t)$ *with a step size* Δ*. Under the Markov Assumption,* $P(X_{lm}^t \mid X_{lm}^{t-1}, z_{1:t-1}, u_{1:t})$ *is equivalent to* $P(X_{lm}^t \mid X_{lm}^{t-1}, u_t)$*.*

We can predict whether the UGV will become stuck at the initial X_{lm} based on data points within the sensor's range, which indicates the presence of obstacles or free space. We use the angle of occupied points which refers to the ratio of the number of occupied points (represented by red dots in Figure 3.2) to the total number of sensor points. A higher ratio suggests that obstacles are present nearby the UGV, increasing the likelihood that the UGV will become trapped at the initial X_{lm}.

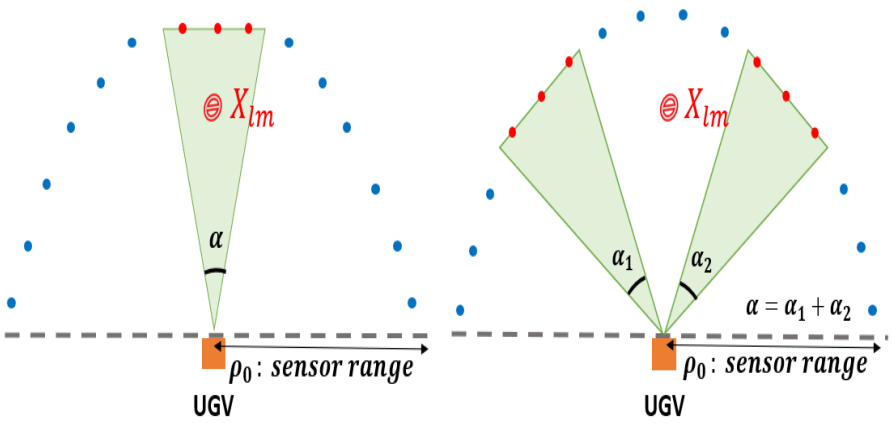

Figure 3.2: Occupied Points Angle.

$$P(X_{lm}^t | X_{lm}^{t-1}, u_t) = \frac{\alpha}{\pi} \tag{3.2}$$

where α is the angle of occupied points in SA(X).

3.2.3 Correction Step

Definition 5 (Observation Likelihood) *The observation likelihood, denoted by* $P(z_t|X_{lm}^t, z_{1:t-1}, u_{1:t})$*, represents the probability of observing the state* X_{lm}^t *given the expected local minima point* (X_{lm}^t)*, the observations* $(z_{1:t-1})$ *and the inputs* $(u_{1:t})$*. This likelihood can be interpreted as the information that the UGV possesses in AOI at time* t*. Under the Markov Assumption,* $P(z_t|X_{lm}^t, z_{1:t-1}, u_{1:t})$ *is equivalent to* $P(z_t|X_{lm}^t)$*.*

$$P(z_t \mid X_{lm}^t = \text{Local Min}) = \frac{\text{RA}(X_t)}{\text{AOI}} \tag{3.3}$$

During the correction step, the prediction $\bar{bel}_t(X_{lm})$ is refined using the recent observation z_t. This refinement involves leveraging the area information that the UGV perceives in AOI in order to identify a local minimum, i.e. the ratio of $\text{RA}(X_t)$ to AOI. This process leads $\bar{bel}_t(X_{lm})$ to an updated posterior belief by multiplying with observation likelihood which represents the probability of the new observation based on the predicted state X_{lm}^t. This adjustment ensures that the belief becomes more accurate by incorporating newly acquired information.

3.2.4 Normalization

In the normalization step, the posterior belief is adjusted to ensure that the total probabilities sum to one, thereby preserving a valid probability distribution. Here, ν represents the normalization factor.

$$\nu = \frac{1}{\text{bel}_t(X_{lm} = \text{not Local Min}) + \text{bel}_t(X_{lm} = \text{Local Min})} \tag{3.4}$$

After the normalization process, the normalized belief $\text{bel}_t(X_{lm} = \text{Local Min})$ is obtained. We use a predefined threshold γ to determine when the UGV should halt its navigation to avoid getting stuck in X_{lm}. If $\text{bel}_t(X_{lm} = \text{Local Min})$ exceeds γ, it implies that the UGV has a confidence level corresponding to $\gamma \times 100\%$ that X_{lm} is a local minimum and is likely to get stuck within a short number of steps. The estimated number of steps before the UGV reaches X_{lm} can be calculated by dividing the distance.

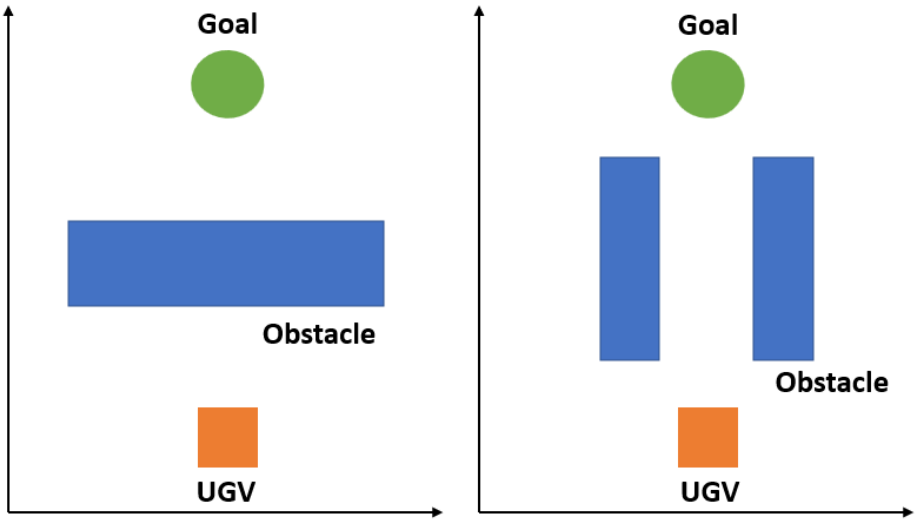

Figure 3.3: Two Occupancy Simulation Environments

3.3 Simulation Environment

Our novel approach was implemented in MATLAB to evaluate its effectiveness. A simulation was created to implement a UGV (represented by an orange box) navigating through an APF field towards a goal location (represented by a green circle). Simulations were conducted in two common scenarios of local minima occurrence for UGVs: Case 1) the UGV is blocked by a long, wall-shaped obstacle and Case 2) the UGV is unable to find a path due to the effects of repulsive forces (see Figure 3.3). We conducted our simulation using a 3D occupancy map that reflects the real-world environment in three dimensions. For sensor representation, we used the rayIntersection function, which provides binary results indicating whether the space is occupied or free in a 3D Occupancy Map, and the distance to the obstacles if they exist.

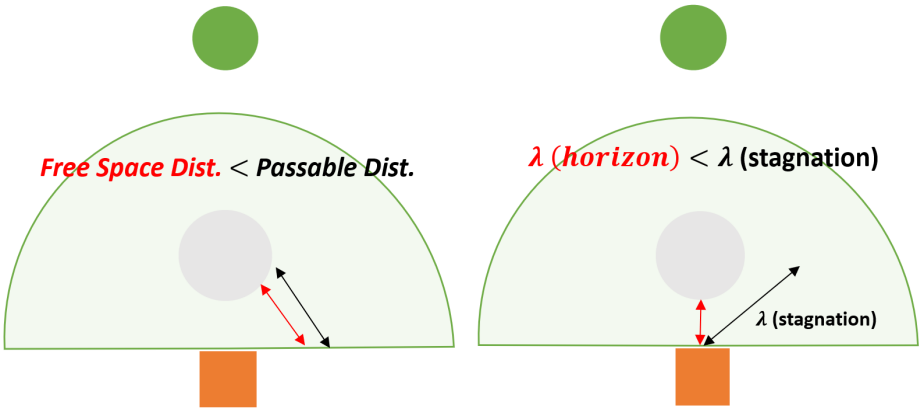

Figure 3.4: Two Comparision Methods. (Method I: Left Figure, Method II: Right Figure)

3.4 Results

3.4.1 Comparison Methods

We compared our methodology with two recent research studies focused on non-convex environments within partially known settings (see Figure 3.4). Method I, to which we compared, predicts the local minimum by examining the distance between adjacent points in the free space in Lidar data. If, within the analyzed range, there is no passage for the robot to navigate through, then the algorithm identifies a local minimum [15]. On the other hand, Method II predicts the local minimum by checking the horizon distance along the extended line of $\vec{F}_{\text{tot}}$ from the robot's position to the nearest obstacle. If the horizon distance λ_{horizon} is less than half of the Lidar's range $\lambda_{\text{stagnation}}$, the algorithm indicates a local minimum prediction [16]. We evaluated whether their algorithms activated in two common local minimum scenarios (see Figure 3.3) and assessed how far in advance they could predict the local minimum (see Table 3.1). Both methods failed to stop in advance or to predict the occurrence of a local minimum. The UGV halts its navigation when it encounters the local minimum at the 108th step in Case 1 and at the 63rd step in Case 2, as defined in Definition 1.

Table 3.1: Results: Comparison Methods

Case 1: a long, wall-shaped obstacle

Metrics	**Method I**	**Method II**
paused_time_step	108	108
local_min prediction	X	X

Case 2: a hallway between two obstacles

Metrics	**Method I**	**Method II**
paused_time_step	63	63
local_min prediction	X	X

3.4.2 A Novel Dynamic Bayesian Filtering Method

Our simulations were conducted under the threshold $\gamma = 0.85$. If $\text{bel}_t(X_{lm} = \text{Local Min})$ exceeds γ, it indicates that the initial X_{lm} is likely to become a local minimum with a probability of 0.85. Our novel approach can predict the local minimum in advance in both scenarios, not only identifying the location of the local minimum but also the number of steps remaining before the UGV reaches the predicted local minimum. In Case 1, our approach can halt the UGV at the 100th step with an 89% confidence level. In addition, in Case 2, the UGV halts its navigation at the 54th step with a 90% confidence level (see Table 3.2). Our earlier prediction of the local minimum enabled the UGV to generate more efficient path planning for subsequent studies, thereby minimizing the total path length to the goal position or reducing the energy consumed for navigation.

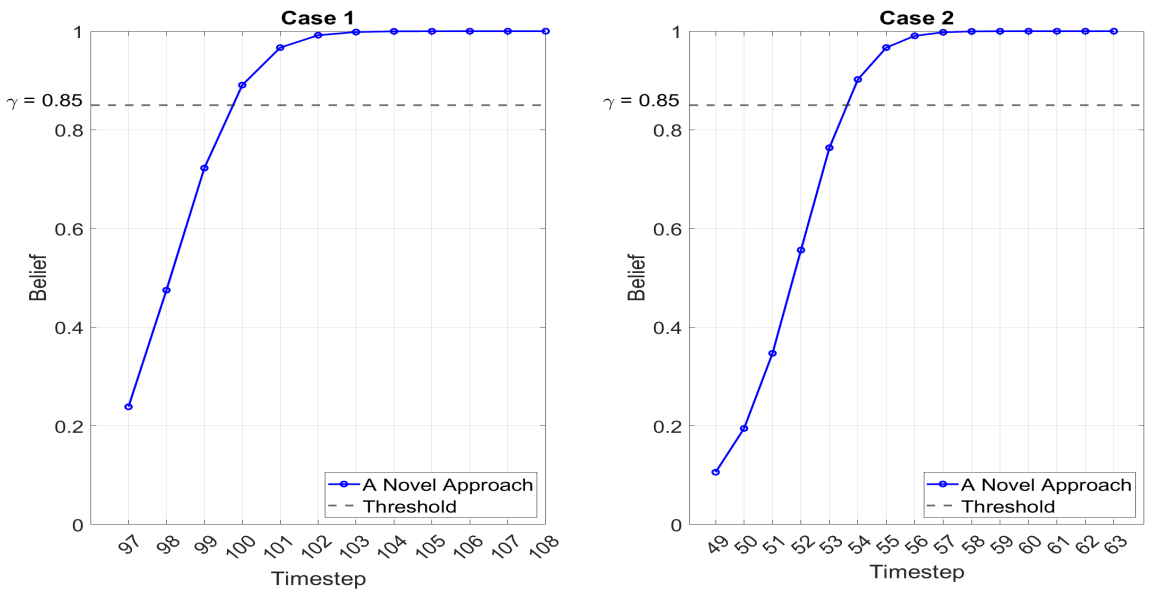

Figure 3.5: Belief in Local Minimum: Two Cases.

Table 3.2: Results: A Novel Approach

Case 1: a long, wall-shaped obstacle

Metrics	**A Novel Approach**
paused_time_step	100
post_belief_minima	0.8908

Case 2: a hallway between two obstacles

Metrics	**A Novel Approach**
paused_time_step	54
post_belief_minima	0.9021

CHAPTER 4

Discussion

4.1 Contributions and Implications

The goal of this thesis was to propose a novel methodology for predicting local minima in local path planning for UGVs. The results demonstrate that our methodology successfully calculates the probability of local minima occurrence, with its accuracy progressively improving over time. This approach offers significant advantages over previously reported methods, particularly in terms of handling uncertainties in unknown environments. First, the UGV can generate local path plans based on raw sensor data. By considering factors such as obstacles, sensor range, and angle, we convert this local information into the probability of the UGV becoming entrapped in local minima. Second, the UGV can update the belief distribution of local minima according to its situational awareness at each time step, which is related to the amount of information the UGV has at each time step. Finally, the new methodology introduced in this paper enables dynamic updates of probabilities without relying on fixed parameters, thereby deriving accurate belief distributions. The UGV can recursively update its state transition probabilities and observation likelihoods based on its current state and local information.

4.2 Limitations and Future Work

A limitation of our study is that our proposed approach to overcome expected local minima has not been fully developed yet. Predicting and then overcoming local minima are crucial steps in path planning because avoiding and bypassing these minima allows us to achieve the objectives of path planning, such as minimizing the overall trajectory or enhancing energy efficiency. Second, although our simulation represents the environment navigated by the UGV in off-road or wilderness settings, it has not been validated with a UGV in real-world environments. Third, to apply this algorithm to a UGV in a real-world environment, we need to integrate the kinematic vehicle model, which accounts for the vehicle's motion. Fourth, the initial belief of a local minimum, which we assumed to follow a uniform distribution, could instead adhere to other distributions with a higher initial probability that reflects the complexity of the environment. Lastly, for time series analysis to be applicable in real-world scenarios, we assumed that observations at each time step are independent, in accordance with the Markov Assumption. However, in real settings, the observation at time t can be correlated with both previous and future time steps.

Future research should focus on employing this novel methodology to prevent the UGV from being trapped in local minima. To overcome the local minimum, we will propose requesting the intervention of a human operator. The UGV can significantly benefit from human intervention since a human operator possesses adaptive and holistic reasoning abilities, influenced by their experiences and knowledge across multiple domains. First, human intervention is requested when $\text{bel}_t(X_{\text{lm}} = \text{Local Min})$ exceeds the threshold (γ), with the predicted positions of local minima being provided. Second, the human operator can be asked to place waypoints, which serve as intermediate goal positions to offset $\vec{F}_{\text{rep}}(t)$ nearby. The human operator can observe the local information where the UGV is located and is likely to get stuck in local minima. Leveraging their knowledge and experience, the human operator provides waypoints that enable the UGV to navigate through areas previously perceived as impassable by the UGV during the local minima prediction stage.

CHAPTER 5

Conclusion

This thesis proposes a novel methodology for predicting local minima based on Dynamic Bayesian Filtering. The advantage of this methodology lies in the UGV's ability to use raw sensor data to predict local minima, while also taking into account the uncertainty due to the unknown area of information in its current state. The results demonstrate that, compared to previous studies, our methodology enables the UGV to predict local minima in advance. Furthermore, the state transition probability from an initial local minimum point enables the UGV to predict subsequent local minima in advance. This not only enhances the post-belief of a local minimum but also allows the UGV to stop earlier with greater confidence. Future work will explore methods for overcoming local minima with human intervention.

APPENDIX A

Dynamic Bayesian Filtering

In this section, the local minimum is denoted by δ.

A.1 Prediction Step

$1.\bar{bel}_t(X_{lm} = \neg\delta)$

$= \{\text{bel}_{t-1}(X_{lm} = \neg\delta) \times P(X_{lm}^t = \neg\delta | X_{lm}^{t-1} = \neg\delta, u_t)\} + \{\text{bel}_{t-1}(X_{lm} = \delta) \times P(X_{lm}^t = \neg\delta | X_{lm}^{t-1} = \delta, u_t)\}$

$= \text{bel}_{t-1}(X_{lm} = \neg\delta) \times \dfrac{\pi - \alpha}{\pi}$

$2.\bar{bel}_t(X_{lm} = \delta)$

$= \{\text{bel}_{t-1}(X_{lm} = \neg\delta) \times P(X_{lm}^t = \delta | X_{lm}^{t-1} = \neg\delta, u_t)\} + \{\text{bel}_{t-1}(X_{lm} = \delta) \times P(X_{lm}^t = \delta | X_{lm}^{t-1} = \delta, u_t)\}$

$= \text{bel}_{t-1}(X_{lm} = \neg\delta) \times \dfrac{\alpha}{\pi} + \text{bel}_{t-1}(X_{lm} = \delta)$

A.2 Correction Step

$$1.bel_t(X_{lm} = \neg\delta)$$

$$= \bar{bel}_t(X_{lm} = \neg\delta) \times P(z_t|X_{lm} = \neg\delta)$$

$$= \bar{bel}_t(X_{lm} = \neg\delta) \times \frac{\mathrm{UA}(X_t)}{\mathrm{AOI}}$$

$$2.bel_t(X_{lm} = \delta)$$

$$= \bar{bel}_t(X_{lm} = \delta) \times P(z_t|X_{lm} = \delta)$$

$$= \bar{bel}_t(X_{lm} = \delta) \times \frac{\mathrm{RA}(X_t)}{\mathrm{AOI}}$$

A.3 Normalization Step

$$1.bel_t(X_{lm} = \neg\delta) = bel_t(X_{lm} = \neg\delta) \times \nu$$

$$2.bel_t(X_{lm} = \delta) = bel_t(X_{lm} = \delta) \times \nu$$

BIBLIOGRAPHY

[1] Omur Arslan and Daniel E Koditschek. Sensor-based reactive navigation in unknown convex sphere worlds. *The International Journal of Robotics Research*, 38(2-3):196–223, 2019.

[2] Farhad Bayat, Sepideh Najafinia, and Morteza Aliyari. Mobile robots path planning: Electrostatic potential field approach. *Expert Systems with Applications*, 100:68–78, 2018.

[3] Sean Campbell, Niall O'Mahony, Anderson Carvalho, Lenka Krpalkova, Daniel Riordan, and Joseph Walsh. Path planning techniques for mobile robots a review. In *2020 6th International Conference on Mechatronics and Robotics Engineering (ICMRE)*, pages 12–16. IEEE, 2020.

[4] Christopher I Connolly. Harmonic functions and collision probabilities. *The International Journal of Robotics Research*, 16(4):497–507, 1997.

[5] Oussama Khatib. Real-time obstacle avoidance for manipulators and mobile robots. *The international journal of robotics research*, 5(1):90–98, 1986.

[6] A Lazarowska. Discrete artificial potential field approach to mobile robot path planning. *IFAC-PapersOnLine*, 52(8):277–282, 2019.

[7] Savvas G Loizou. Closed form navigation functions based on harmonic potentials. In *2011 50th IEEE Conference on Decision and Control and European Control Conference*, pages 6361–6366. IEEE, 2011.

[8] Ahmad A Masoud. A harmonic potential field approach with a probabilistic space descriptor for planning in non-divisible environments. In *2009 IEEE International Conference on Robotics and Automation*, pages 3774–3779. IEEE, 2009.

[9] Ulises Orozco-Rosas, Oscar Montiel, and Roberto Sepúlveda. Mobile robot path planning using membrane evolutionary artificial potential field. *Applied Soft Computing*, 77:236–251, 2019.

[10] Panagiotis Papadakis. Terrain traversability analysis methods for unmanned ground vehicles: A survey. *Engineering Applications of Artificial Intelligence*, 26(4):1373–1385, 2013.

[11] Santiago Paternain, Daniel E Koditschek, and Alejandro Ribeiro. Navigation functions for convex potentials in a space with convex obstacles. *IEEE Transactions on Automatic Control*, 63(9):2944–2959, 2017.

[12] Jose Ricardo Sanchez-Ibanez, Carlos J Perez-del Pulgar, and Alfonso García-Cerezo. Path planning for autonomous mobile robots: A review. *Sensors*, 21(23):7898, 2021.

[13] Simo Särkkä and Lennart Svensson. *Bayesian filtering and smoothing*, volume 17. Cambridge university press, 2023.

[14] Mayur Sawant, Soulaimane Berkane, Ilia Polushin, and Abdelhamid Tayebi. Hybrid feedback for autonomous navigation in planar environments with convex obstacles. *IEEE Transactions on Automatic Control*, 2023.

[15] Rafal Szczepanski, Artur Bereit, and Tomasz Tarczewski. Efficient local path planning algorithm using artificial potential field supported by augmented reality. *Energies*, 14(20):6642, 2021.

[16] Rafal Szczepanski, Tomasz Tarczewski, and Krystian Erwinski. Energy efficient local path planning algorithm based on predictive artificial potential field. *IEEE Access*, 10:39729–39742, 2022.

[17] Vasileios Vasilopoulos and Daniel E Koditschek. Reactive navigation in partially known non-convex environments. In *International Workshop on the Algorithmic Foundations of Robotics*, pages 406–421. Springer, 2018.

[18] Qingfeng Yao, Zeyu Zheng, Liang Qi, Haitao Yuan, Xiwang Guo, Ming Zhao, Zhi Liu, and Tianji Yang. Path planning method with improved artificial potential field—a reinforcement learning perspective. *IEEE Access*, 8:135513–135523, 2020.

[19] Ekim Yurtsever, Jacob Lambert, Alexander Carballo, and Kazuya Takeda. A survey of autonomous driving: Common practices and emerging technologies. *IEEE access*, 8:58443–58469, 2020.